Mathematics

http://www.aimspress.com/journal/Math

AIMS Mathematics, 9(4): 9211–9231.
DOI: 10.3934/math.2024449
Received: 14 January 2024
Revised: 23 February 2024
Accepted: 28 February 2024
Published: 06 March 2024

Research article

Event-triggered fixed/preassigned time stabilization of state-dependent switching neural networks with mixed time delays

Jiashu Gao[1], **Jing Han**[2] **and Guodong Zhang**[1,*]

[1] College of Mathematics and Statistics, South-Central Minzu University, Wuhan 430074, China
[2] School of Information Engineering, Wuhan Business University, Wuhan 430056, China

* **Correspondence:** Email: zgd2008@mail.scuec.edu.cn.

Abstract: This study employed an event-triggered control (ETC) strategy to investigate the problems of fixed-time stabilization (FTS) and preassigned-time stabilization (PTS) for state-dependent switching neural networks (SDSNNs) that involved mixed time delays. To enhance the network's generalization capability and accelerate convergence stabilization, a more intricate weight-switching mechanism was introduced, then to mitigate transmission energy consumption, this paper proposed a tailored event-triggering rule that triggered the ETC solely at predetermined time points. This rule ensured the stability of the system while effectively reducing energy consumption. Using the Lyapunov stability theory and various inequality techniques, this paper presented new results for FTS and PTS of SDSNNs. The validity of these findings was supported by conducting data simulations in two illustrative examples.

Keywords: fixed/preassigned-time stabilization; event-triggered control; state-dependent switching; mixed time delays
Mathematics Subject Classification: 34H15, 34K34

1. Introduction

Based on research in modern neuroscience [1], neural networks have gained attention due to their ability to simulate the structural characteristics of the human brain. After being activated by external stimuli, the synaptic connection weights of neurons can be adjusted to facilitate information transmission between neurons; therefore, a large number of circuit components are constructed to support this transmission. When facing practical applications that require processing large-scale datasets, the complex computations and the transmission of a vast amount of data result in catastrophic power consumption and storage usage.

Memristors [2, 3], due to their non-volatility and the ability to continuously change their resistance states, can effectively exhibit the plasticity of neural synapses. They are gradually replacing traditional resistors in the design of artificial neural networks and have been widely applied in simulating the human brain [4]. In the research, memristors are utilized as state switching elements to achieve internal state switching in neural networks by adjusting the resistance values of memristors. As a result, the state-dependent switching neural networks (SDSNNs) were constructed [5]. A state switching system is typically composed of transition rules between several discrete states through which the system's behavior and evolution are described. In neural networks, this switching mode exhibits significant advantages in processing dynamic data and reducing the high power consumption and storage caused by signal transmission. Consequently, they have found widespread applications in diverse fields, including speech recognition [6], intelligent control [7], and fault diagnosis [8].

Undoubtedly, the significance of stability in nonlinear systems [9–13] is widely recognized. Compared to the conventional notion of asymptotic stability, finite-time stability possesses superior performance advantages, which has attracted extensive research attention from many researchers. The relevant finite-time stability results of SDSNNs have been presented in [14–16]. However, due to the dependency of finite-time stability on initial conditions, the precise acquisition of initial conditions remains a major challenge in practical applications. Therefore, considering this limitation, we introduce the concept of fixed-time stability (FTS) to address this issue [17].

In FTS, the settling-time is dictated by designing the control strategy and parameters, and is independent of the initial conditions. The system must converge to a stable state within a fixed time. Under its own strict and robust stability requirements, FTS has significant application value for control problems that demand high precision and response speed, such as aerospace engineering, robot control, and intelligent transportation. The research on FTS has attracted increasing attention and has become a vital research area in contemporary control theory and applications [18–22].

Nonetheless, FTS sets time as a parameter or hyperparameter in the model, which restricts its capability to flexibly learn the relationship between time and other features. To address this limitation, our study proposes the concept of preassigned-time stabilization (PTS), whereby time is considered an input feature alongside other features provided to the neural network model; thus, time is no longer considered as a static, immutable parameter but rather as a dynamic factor that allows for future data prediction. PTS necessitates swift convergence the system to a stable state within a predefined time, indicating that the control system can achieve fast stabilization at any moment and exhibits stronger robustness against external disturbances and parameter fluctuations; therefore, PTS offers more stringent performance guarantees. PTS has been employed in numerous studies on stabilization and synchronization, showcasing encouraging outcomes [23, 24]. When confronted with requirements for real-time performance and safety, PTS can present an effective method and guide principles for devising more efficient, rapid, and precise control systems.

Traditional control methods rely on continuous control inputs to ensure system performance, which requires a significant amount of communication resources to transmit control signals. In contrast, event-triggered control (ETC) only triggers sampling and control actions when specific events occur by monitoring changes in system states or errors. By designing event-triggering rules appropriately, it is possible to flexibly meet the practical control requirements.

With the increasing attention to ETC, numerous researchers have made significant achievements around event triggering strategies [5, 20, 21, 25–29]. Among these studies, event-triggering strategies have been successfully applied to neural networks with state switches in [5, 21, 25–29]. In 2022, Li et al. [30] introduced a more concise lemma for demonstrating the FTS of systems. In 2022, Li et al. [24] examined the fixed and preassigned-time stabilization of SDSNNs incorporating time delays. In 2023, Zhang [20] developed a novel and effective ETC technique for achieving fixed-time synchronization and stabilization. Based on the above discussions, the objective of this paper is to tackle the fixed/preassigned-time stabilization problem of neural networks with mixed delays in state switches through ETC. The innovations of this paper are summarized as follows:

1) Differing from the models in [23, 28, 29] that employ simple switch of connection weights, the model proposed in this paper adopts a more complex switching mechanism in the form of differentiable switches. Results obtained under this switching mode are more generalizable and enable the network to exhibit superior performance when handling unknown data.

2) Despite the extensive results presented in [5, 14, 15, 18–20, 25, 31] on the traditional asymptotic stability, finite-time or fixed-time stabilization of switched systems, there has been no such study for the model in this paper. This paper discusses fixed/preassigned-time stabilization, filling this research gap and enriching the results for achieving stabilization, thereby enhancing the efficiency and precision of the system.

3) Compared to [32], which only employs mixed delays, this paper proposes an ETC strategy based on mixed delays. This strategy eliminates the need for the system to remain in a control state at all times, thus effectively saving communication resources. The proposed control strategy is more widely applicable and can be easily extended to higher-order, complex-valued, and quaternion-valued domains.

The remaining parts have the following structures: Section 2 covers the preliminaries. In Section 3, the main results of this paper about FTS and PTS are disclosed. Simulations and comparisons are displayed in Section 4. Finally, some conclusions are given in Section 5.

Notation: In this paper, the solutions of all systems are considered in Filippov's sense [33]. $\mathrm{co}[\delta^{\flat}, \delta^{\flat\flat}]$ denotes the convex hull of $\{\delta^{\flat}, \delta^{\flat\flat}\}$.

$$\overline{\jmath}_s = \max\{\jmath_s^{\flat},\ \jmath_s^{\flat\flat}\}, \quad \underline{\jmath}_s = \min\{\jmath_s^{\flat},\ \jmath_s^{\flat\flat}\}, \quad \overline{a}_{sz} = \max\{a_{sz}^{\flat},\ a_{sz}^{\flat\flat}\}, \quad \underline{a}_{sz} = \min\{a_{sz}^{\flat},\ a_{sz}^{\flat\flat}\},$$
$$\overline{b}_{sz} = \max\{b_{sz}^{\flat},\ b_{sz}^{\flat\flat}\}, \quad \underline{b}_{sz} = \min\{b_{sz}^{\flat},\ b_{sz}^{\flat\flat}\}, \quad a_{sz}^{max} = \max\{|\underline{a}_{sz}|, |\overline{a}_{sz}|\}, \quad b_{sz}^{max} = \max\{|\underline{b}_{sz}|, |\overline{b}_{sz}|\},$$
$$c_{sz}^{max} = \max\{|\underline{c}_{sz}|, |\overline{c}_{sz}|\}, \quad c_{sz}^{min} = \min\{|\underline{c}_{sz}|, |\overline{c}_{sz}|\}, \quad s, z \in \mathcal{W} = \{1, 2, \cdots, \hbar\}.$$

2. Preliminaries

The SDSNNs with mixed delays are

$$\begin{aligned}\frac{\mathrm{d}\chi_s(t)}{\mathrm{d}t} =& -\jmath_s(\chi_s(t))\chi_s(t) + \sum_{z=1}^{\hbar} a_{sz}(\chi_s(t))\Im_z(\chi_z(t)) + \sum_{z=1}^{\hbar} b_{sz}(\chi_s(t))\Im_z(\chi_z(t-\tau_z(t)))\\ &+ \sum_{z=1}^{\hbar} c_{sz}(\chi_s(t)) \int_{t-r_z(t)}^{t} \Im_z(\chi_z(\upsilon))\mathrm{d}\upsilon, \quad t \geq 0, s \in \mathcal{W},\end{aligned} \tag{1}$$

with the initial values as

$$\chi(\upsilon) = (\chi_1(\upsilon), \chi_2(\upsilon), \cdots, \chi_{\hbar}(\upsilon))^T \in C([-h, 0], \mathbb{R}),$$

in which

$$h = \max\{\tau, r\}, \quad \chi(t) = (\chi_1(t), \cdots, \chi_\hbar(t))^T \in \mathbb{R}^n$$

is state variable, $\jmath_s(\chi_s(t))$ is self-feedback weight, $a_{sz}(\chi_s(t)), b_{sz}(\chi_s(t)), c_{sz}(\chi_s(t))$ are memristor-based weights, $f_s(\cdot)$ is a nonlinear activation function, $\tau_z(\cdot)$ is discrete time-varying delays, where $\tau_z(\cdot) < \tau_z$, τ_z is a constant, and $r_z(\cdot)$ is distributed time-varying delays, $0 \leqslant r_z(t) \leqslant r_z$, $\dot{r}_z(t) \leqslant h$, in which $\tau_z, h < 1$ are constants above $s, z \in \mathcal{W}$.

Based on the previous work [34], it is expected that the state-dependent parameters in (1) fulfill the following conditions:

$$\begin{aligned}
\jmath_s(\chi_s(t)) &= \begin{cases} \jmath_s^{\flat}, & -\frac{\mathrm{d}\Im_s(\chi_s(t))}{\mathrm{d}t} \le \frac{\mathrm{d}\chi_s(t)}{\mathrm{d}t}, \\ \jmath_s^{\flat\flat}, & -\frac{\mathrm{d}\Im_s(\chi_s(t))}{\mathrm{d}t} > \frac{\mathrm{d}\chi_s(t)}{\mathrm{d}t}, \end{cases} \\
a_{sz}(\chi_s(t)) &= \begin{cases} a_{sz}^{\flat}, & \varrho_{sz}\frac{\mathrm{d}\Im_z(\chi_z(t))}{\mathrm{d}t} \le \frac{\mathrm{d}\chi_s(t)}{\mathrm{d}t}, \\ a_{sz}^{\flat\flat}, & \varrho_{sz}\frac{\mathrm{d}\Im_z(\chi_z(t))}{\mathrm{d}t} > \frac{\mathrm{d}\chi_s(t)}{\mathrm{d}t}, \end{cases} \\
b_{sz}(\chi_s(t)) &= \begin{cases} b_{sz}^{\flat}, & \varrho_{sz}\frac{\mathrm{d}\Im_z(\chi_z(t-\tau_z(t)))}{\mathrm{d}t} \le \frac{\mathrm{d}\chi_s(t)}{\mathrm{d}t}, \\ b_{sz}^{\flat\flat}, & \varrho_{sz}\frac{\mathrm{d}\Im_z(\chi_z(t-\tau_z(t)))}{\mathrm{d}t} > \frac{\mathrm{d}\chi_s(t)}{\mathrm{d}t}, \end{cases} \\
c_{sz}(\chi_s(t)) &= \begin{cases} c_{sz}^{\flat}, & \varrho_{sz}\{\Im_z(\chi_z(t)) - \Im_z(\chi_z(t-r_z(t)))\} \le \frac{\mathrm{d}\chi_s(t)}{\mathrm{d}t}, \\ c_{sz}^{\flat\flat}, & \varrho_{sz}\{\Im_z(\chi_z(t)) - \Im_z(\chi_z(t-r_z(t)))\} > \frac{\mathrm{d}\chi_s(t)}{\mathrm{d}t}, \end{cases}
\end{aligned} \tag{2}$$

where $\jmath_s^{\flat}, \jmath_s^{\flat\flat}, a_{sz}^{\flat}, a_{sz}^{\flat\flat}, b_{sz}^{\flat}, b_{sz}^{\flat\flat}, c_{sz}^{\flat}, c_{sz}^{\flat\flat}$ are constant numbers, $s, z \in \mathcal{W} = \{1, 2, \cdots, \hbar\}$, and $\varrho_{sz} = 1$, if $s \neq z$ holds; otherwise, -1.

To achieve FTS and PTS of system (3), we consider the following stabilization system:

$$\begin{aligned}
\frac{\mathrm{d}\chi_s(t)}{\mathrm{d}t} =& - \jmath_s(\chi_s(t))\chi_s(t) + \sum_{z=1}^{\hbar} a_{sz}(\chi_s(t))\Im_z(\chi_z(t)) + \sum_{z=1}^{\hbar} b_{sz}(\chi_s(t))\Im_z(\chi_z(t-\tau_z(t))) \\
&+ \sum_{z=1}^{\hbar} c_{sz}(\chi_s(t)) \int_{t-r_z(t)}^{t} \Im_z(\chi_z(\upsilon))\mathrm{d}\upsilon + u_s(t), \quad t \ge 0, s \in \mathcal{W}.
\end{aligned} \tag{3}$$

Remark 1. The switching condition for defining parameters $\jmath_s(\chi_s(t)), a_{sz}(\chi_s(t)), b_{sz}(\chi_s(t)), c_{sz}(\chi_s(t))$ is determined by the state of the neurons, and $u_s(t)$ is the controller.

By utilizing the theory of differential inclusion [33] and set-valued mapping, we know that

$$\begin{aligned}
\frac{\mathrm{d}\chi_s(t)}{\mathrm{d}t} \in& - \mathrm{co}[\jmath_s(\chi_s(t))]\chi_s(t) + \sum_{z=1}^{\hbar} \mathrm{co}[a_{sz}(\chi_s(t))]\Im_z(\chi_z(t)) + \sum_{z=1}^{\hbar} \mathrm{co}[b_{sz}(\chi_s(t))]\Im_z(\chi_z(t-\tau_z(t)) \\
&+ \sum_{z=1}^{\hbar} \mathrm{co}[c_{sz}(\chi_s(t)] \int_{t-r_z(t)}^{t} \Im_z(\chi_z(\upsilon))\mathrm{d}\upsilon + \mathrm{co}[u_s(t)], \text{ for a.e. } t \ge 0, s \in \mathcal{W},
\end{aligned} \tag{4}$$

where

$$\mathrm{co}[\jmath_s(\chi_s(t))] = \begin{cases} \jmath_s^{\flat}, & -\frac{\mathrm{d}\Im_s(\chi_s(t))}{\mathrm{d}t} \le \frac{\mathrm{d}\chi_s(t)}{\mathrm{d}t}, \\ \left[\underline{\jmath}_s, \bar{\jmath}_s\right], & -\frac{\mathrm{d}\Im_s(\chi_s(t))}{\mathrm{d}t} = \frac{\mathrm{d}\chi_s(t)}{\mathrm{d}t}, \\ \jmath_s^{\flat\flat}, & -\frac{\mathrm{d}\Im_s(\chi_s(t))}{\mathrm{d}t} > \frac{\mathrm{d}\chi_s(t)}{\mathrm{d}t}, \end{cases}$$

$$\text{co}[a_{sz}(\chi_s(t))] = \begin{cases} a^{\flat}_{sz}, & \varrho_{sz}\frac{\mathrm{d}\Im_z(\chi_z(t))}{\mathrm{d}t} \le \frac{\mathrm{d}\chi_s(t)}{\mathrm{d}t}, \\ \left[\underline{a}_{sz}, \overline{a}_{sz}\right], & \varrho_{sz}\frac{\mathrm{d}\Im_z(\chi_z(t))}{\mathrm{d}t} = \frac{\mathrm{d}\chi_s(t)}{\mathrm{d}t}, \\ a^{\flat\flat}_{sz}, & \varrho_{sz}\frac{\mathrm{d}\Im_z(\chi_z(t))}{\mathrm{d}t} > \frac{\mathrm{d}\chi_s(t)}{\mathrm{d}t}, \end{cases}$$

$$\text{co}[b_{sz}(\chi_s(t))] = \begin{cases} b^{\flat}_{sz}, & \varrho_{sz}\frac{\mathrm{d}\Im_z(\chi_z(t-\tau_z(t)))}{\mathrm{d}t} \le \frac{\mathrm{d}\chi_s(t)}{\mathrm{d}t}, \\ \left[\underline{b}_{sz}, \overline{b}_{sz}\right], & \varrho_{sz}\frac{\mathrm{d}\Im_z(\chi_z(t-\tau_z(t)))}{\mathrm{d}t} = \frac{\mathrm{d}\chi_s(t)}{\mathrm{d}t}, \\ b^{\flat\flat}_{sz}, & \varrho_{sz}\frac{\mathrm{d}\Im_z(\chi_z(t-\tau_z(t)))}{\mathrm{d}t} > \frac{\mathrm{d}\chi_s(t)}{\mathrm{d}t}, \end{cases}$$

$$\text{co}[c_{sz}(\chi_s(t))] = \begin{cases} c^{\flat}_{sz}, & \varrho_{sz}\{\Im_z(\chi_z(t)) - \Im_z(\chi_z(t-r_z(t)))\} \le \frac{\mathrm{d}\chi_s(t)}{\mathrm{d}t}, \\ \left[\underline{c}_{sz}, \overline{c}_{sz}\right], & \varrho_{sz}\{\Im_z(\chi_z(t)) - \Im_z(\chi_z(t-r_z(t)))\} = \frac{\mathrm{d}\chi_s(t)}{\mathrm{d}t}, \\ c^{\flat\flat}_{sz}, & \varrho_{sz}\{\Im_z(\chi_z(t)) - \Im_z(\chi_z(t-r_z(t)))\} > \frac{\mathrm{d}\chi_s(t)}{\mathrm{d}t}. \end{cases} \tag{5}$$

By using measurable selection theory [33], we know that there exist

$$\jmath_s(t) \in \text{co}[\jmath_{sz}(\chi_s(t))], \quad a_{sz}(t) \in \text{co}[a_{sz}(\chi_s(t))], \quad b_{sz}(t) \in \text{co}[b_{sz}(\chi_s(t))], \quad c_{sz}(t) \in \text{co}[c_{sz}(\chi_s(t))]$$

and

$$\breve{u}_s(t) \in \text{co}[u_s(t)],$$

such that

$$\frac{\mathrm{d}\chi_s(t)}{\mathrm{d}t} = -\jmath_s(t)\chi_s(t) + \sum_{z=1}^{\hbar} a_{sz}(t)\Im_z(\chi_z(t)) + \sum_{z=1}^{\hbar} b_{sz}(t)\Im_z(\chi_z(t-\tau_z(t)) + \sum_{z=1}^{\hbar} c_{sz}(t)\int_{t-r_z(t)}^{t} \Im_z(\chi_z(\upsilon))\mathrm{d}\upsilon + \breve{u}_s(t), \text{ for a.e. } t \ge 0, s \in \mathcal{W}. \tag{6}$$

Assumption 1. The feedback function $\Im_z(\cdot)$, $z = 1, 2, \cdots, \hbar$ is bounded, there exists a number M such that $|\Im_z(\cdot)| \le M$, and it satisfies the condition $\Im_z(0) = 0$.

Definition 1. [28] For any $\chi_0 = \chi(0) \in \mathbb{R}^n$, let

$$T(\chi_0) = \{t^* : \chi(t) = 0, \forall t > t^*\}$$

be the settling time function. If there exists a constant $T_{max} > 0$, such that $T(\chi(0)) \le T_{max}$ for any $\chi(0) \in \mathbb{R}^n$, and if

$$\lim_{t \to T_{max}} \|\chi(\upsilon)\| = 0$$

holds, then the system (3) is called FTS and T_{max} is called setting-time.

Definition 2. [35] If there exists a preassigned constant $T_p > 0$, such that the function $T(\chi(0)) \le T_p$ for any $\chi(0) \in \mathbb{R}^n$, and if

$$\lim_{t \to T_p} \|\chi(\upsilon)\| = 0$$

holds, then the system (3) is called PTS and T_p is called preassigned-time.

For deriving the main results, the following lemmas are needed.

Lemma 1. [36] Let $\pi_s \geq 0, (s = 1, 2, \cdots, \hbar), 0 < p_1 \leq 1$, and $p_2 \geq 1$; one has

$$\sum_{s=1}^{\hbar} \pi_s^{p_1} \geq (\sum_{s=1}^{\hbar} \pi_s)^{p_1}, \sum_{s=1}^{\hbar} \pi_s^{p_2} \geq \hbar^{1-p_2}(\sum_{s=1}^{\hbar} \pi_s)^{p_2}.$$

Lemma 2. [30, 37] There exists a continuous, positive-definite, and radically unbounded function

$$V(y(t)) : \mathbb{R}^n \to \mathbb{R}, y(t) = 0 \Leftrightarrow V(y(t)) = 0,$$

such that any solution $y(t)$ of system (6) satisfies the inequality

$$\frac{\mathrm{d}V(y(t))}{\mathrm{d}t} \leq \begin{cases} -\zeta V(y(t)) - \mathfrak{R}_1 V^{\omega}(y(t)), \ if V(y(t)) \in (0, 1), \\ -\zeta V(y(t)) - \mathfrak{R}_2 V^{\omega}(y(t)), \ if V(y(t)) \geq 1, \end{cases}$$

where

$$\zeta > 0, \ \mathfrak{R}_1 > 0, \ \mathfrak{R}_2 > 0, \ \zeta < \min\{\mathfrak{R}_1, \mathfrak{R}_2\}, \ \omega = \lambda + sign(V(y(t)) - 1), \ 1 < \lambda < 2.$$

The settling-time of FTS is

$$T_{max} = \frac{1}{\zeta(\lambda - 2)} \ln \frac{\mathfrak{R}_1}{\mathfrak{R}_1 + \zeta} - \frac{1}{\lambda\zeta} \ln \frac{\mathfrak{R}_2}{\mathfrak{R}_2 + \zeta}.$$

Lemma 3. If there exists a continuous, positive-definite, and radically unbounded function

$$V(y(t)) : \mathbb{R}^n \to \mathbb{R}, \quad y(t) = 0 \Leftrightarrow V(y(t)) = 0,$$

such that any solution $y(t)$ of system (6) satisfies the inequality

$$\frac{\mathrm{d}V(y(t))}{\mathrm{d}t} \leq \frac{T_{max}}{T_p}(-\zeta V(y(t)) - \mathfrak{R} V^{\omega}(y(t))),$$

then the origin of SDSNNs (3) is PTS within setting-time T_{max} and preassigned-time T_p, in which

$$T_{max} = \frac{1}{\zeta(\lambda - 2)} \ln \frac{\mathfrak{R}}{\mathfrak{R} + \zeta} - \frac{1}{\lambda\zeta} \ln \frac{\mathfrak{R}}{\mathfrak{R} + \zeta},$$

where other parameters are the same as in Lemma 2.

Remark 2. Based on the FTS lemma provided in [30], this paper establishes Lemma 2 while ensuring the condition -$\zeta < 0$ in the inequality

$$\frac{\mathrm{d}V(y(t))}{\mathrm{d}t} \leq -\zeta V(y(t)) - \mathfrak{R} V^{\omega}(y(t)).$$

Building upon this lemma, the paper extends its findings and introduces a new PTS lemma, namely Lemma 3.

Remark 3. Many previous studies have focused on FTS [18–24], with some PTS results provided in the researches [23,24,35]. However, these systems often do not involve state switching, and the controllers do not utilize ETC. In comparison to the main systems incorporating state switching [4, 14, 15, 18, 19], this paper optimizes the model's state switching by employing derivative-enhanced complex switching, resulting in more general outcomes. Additionally, an ETC strategy is implemented to reduce power consumption. For the model in this paper, FTS and PTS results have not been studied yet, therefore, this paper will supplement the following content.

3. Main results

3.1. FTS of SDSNNs (3)

Let controller $\breve{u}_s(t)$, $s \in \mathcal{W}$ in system (6) be

$$\breve{u}_{1s}(t) = -\rho_s\chi_s(t_\iota) - \sigma_s[\chi_s^2(t_\iota)]^{\omega-1}\chi_s(t_\iota) - \kappa_s\phi_s(t_\iota), \quad t \in [t_\iota, t_{\iota+1}), \iota = 1, 2, \cdots, \tag{7}$$

in which $\rho_s, \sigma_s, \kappa_s$ are all positive constants,

$$\omega = \lambda + sign(V(t) - 1)$$

for $t \in [t_\iota, t_{\iota+1})$, $1 < \lambda < 2$,

$$\phi_s(t) \in \text{co}[(sign(\chi_s(t))]$$

and

$$\text{V}(t) = \sum_{s=1}^{\hbar}\chi_s^2(t).$$

Let

$$\breve{\mathcal{U}}_{1s}(t) = -\rho_s\chi_s(t) - \sigma_s[\chi_s^2(t)]^{\omega-1}\chi_s(t) - \kappa_s\phi_s(t).$$

The measure error is

$$\mathcal{E}_{1s}(t) = \breve{\mathcal{U}}_{1s}(t) - \breve{u}_{1s}(t)$$

and event-triggering is

$$t_{\iota+1} = \{t|t > t_\iota, |\mathcal{E}_{1s}(t)| \geq \varsigma_s|\chi_s(t)| + \alpha_s\sigma_s|\chi_s^{2\omega-1}(t)| + \gamma_s(1 - \vartheta_s)^t\}, \tag{8}$$

where $\alpha_s, \vartheta_s \in (0, 1), \varsigma_s, \gamma_s > 0$, and t_ι ($\iota = 0, 1, 2, \cdots, s \in \mathbb{N}$) is the ι th triggering instant.

Let

$$\kappa_s \geq \sum_{z=1}^{\hbar} a_{sz}^{max}M + \sum_{z=1}^{\hbar} b_{sz}^{max}M + \sum_{z=1}^{\hbar} c_{sz}^{max}Mr_z + \gamma_s, \tag{9}$$

$$\zeta_s = 2(J_s^{min} + \rho_s - \varsigma_s), \quad s \in \mathcal{W}. \tag{10}$$

The main results of this subsection are presented as follows.

Theorem 1. Under Assumption 1, Lemma 2, and ETC (7) and (8), if (9) and $\zeta_s > 0$ ($s \in \mathcal{W}$) hold, SDSNNs (3) get FTS and the settling-time is T_{max}.

Proof. Now, we construct a Lyapunov functional:

$$\text{V}(t) = \sum_{s=1}^{\hbar}\chi_s^2(t). \tag{11}$$

For $t \in [t_\iota, t_{\iota+1})$, $\iota = 1, 2, \cdots$, by using the properties of C-regular functions [38] and taking the derivative of V(t) with respect to any solutions of (6), we obtain

$$\begin{aligned}\frac{\mathrm{d}V(t)}{\mathrm{d}t} =& 2\sum_{s=1}^{\hbar}\chi_s(t)\cdot\frac{\mathrm{d}\chi_s(t)}{\mathrm{d}t}\\ =& 2\sum_{s=1}^{\hbar}\chi_s(t)[-\jmath_s(t)\chi_s(t)+\sum_{z=1}^{\hbar}a_{sz}(t)\Im_z(\chi_z(t))+\sum_{z=1}^{\hbar}b_{sz}(t)\Im_z(\chi_z(t-\tau_z(t)))\\ &+\sum_{z=1}^{\hbar}c_{sz}(t)\int_{t-r_z(t)}^{t}\Im_z(\chi_z(\upsilon))\mathrm{d}\upsilon+\breve{u}_{1s}(t)]\\ \le& 2\sum_{s=1}^{\hbar}[-\jmath_s(t)\chi_s^2(t)+\sum_{z=1}^{\hbar}a_{sz}(t)|\chi_s(t)||\Im_z(\chi_z(t))|+\sum_{z=1}^{\hbar}b_{sz}(t)|\chi_s(t)||\Im_z(\chi_z(t-\tau_z(t))|\\ &+\sum_{z=1}^{\hbar}c_{sz}(t)|\chi_s(t)|\int_{t-r_z(t)}^{t}|\Im_z(\chi_z(\upsilon))|\mathrm{d}\upsilon+\breve{u}_{1s}(t)\chi_s(t)].\end{aligned}\tag{12}$$

From (7) and (12), one obtains

$$\begin{aligned}\frac{\mathrm{d}V(t)}{\mathrm{d}t} \le& 2\sum_{s=1}^{\hbar}[-\jmath_s^{min}\chi_s^2(t)+\sum_{z=1}^{\hbar}a_{sz}^{max}M|\chi_s(t)|+\sum_{z=1}^{\hbar}b_{sz}^{max}M|\chi_s(t)|\\ &+\sum_{z=1}^{\hbar}c_{sz}^{max}r_zM|\chi_s(t)|+\phi_s(t)\chi_s(t)(\breve{\mathcal{U}}_{1s}(t)-\mathcal{E}_{1s}(t))]\\ \le& 2\sum_{s=1}^{\hbar}(-\jmath_s^{min}-\rho_s+\varsigma_s)\chi_s^2(t)+2\sum_{s=1}^{\hbar}|\chi_s(t)|[\sum_{z=1}^{\hbar}a_{sz}^{max}M+\sum_{z=1}^{\hbar}b_{sz}^{max}M\\ &+\sum_{z=1}^{\hbar}c_{sz}^{max}r_zM-\kappa_s+\gamma_s]-2\sum_{s=1}^{\hbar}[\chi_s^2(t)]^{\omega}(\sigma_s-\alpha_s\sigma_s)\\ &+2\sum_{s=1}^{\hbar}|\chi_s(t)|[|\mathcal{E}_{1s}(t)|-\varsigma_s|\chi_s(t)|-\alpha_s\sigma_s|\chi_s^{2\omega-1}(t)|-\gamma_s(1-\vartheta_s)^t].\end{aligned}\tag{13}$$

By using conditions (8)–(10), one knows that

$$\frac{\mathrm{d}V(t)}{\mathrm{d}t}\le\sum_{s=1}^{\hbar}(-\zeta_s\chi_s^2(t)-2(1-\alpha_s)\sigma_s[\chi_s^2(t)]^{\omega}).\tag{14}$$

Utilizing Lemma 1 in [36], one can derive

(1) If $V(t)\in(0,1)$,

$$\begin{aligned}-\sum_{s=1}^{\hbar}2(1-\alpha_s)\sigma_s[\chi_s^2(t)]^{\omega}\le& -\mathfrak{R}_1\sum_{s=1}^{\hbar}[\chi_s^2(t)]^{\omega}\\ =& -\mathfrak{R}_1V^{\omega}(t),\end{aligned}\tag{15}$$

in which

$$\mathfrak{R}_1 = min_{s\in\mathcal{W}}\{2(1-\alpha_s)\sigma_s\}.$$

(2) If $V(t) \geq 1$,

$$-\sum_{s=1}^{\hbar} 2(1-\alpha_s)\sigma_s[\chi_s^2(t)]^{\omega} \leq -\mathfrak{R}_2\sum_{s=1}^{\hbar}[\chi_s^2(t)]^{\omega} = -\mathfrak{R}_2 V^{\omega}(t), \tag{16}$$

where $\mathfrak{R}_2 = \mathfrak{R}_1\hbar^{-\lambda}$. From (13)–(16), one obtains

$$\frac{\mathrm{d}V(y(t))}{\mathrm{d}t} \leq \begin{cases} -\zeta V(y(t)) - \mathfrak{R}_1 V^{\omega}(y(t)),\ if\ V(y(t)) \in (0,1), \\ -\zeta V(y(t)) - \mathfrak{R}_2 V^{\omega}(y(t)),\ if\ V(y(t)) \geq 1, \end{cases} \tag{17}$$

where

$$\zeta = min_{s\in\mathcal{W}}\{\zeta_s\}, \quad \zeta < min\{\mathfrak{R}_1, \mathfrak{R}_2\}.$$

From Definition 1 and Lemma 2, we get SDSNNs (3) to achieve FTS at the settling-time T_{max}. The proof is finished. □

Theorem 2. The system (6) does not have Zeno-behavior with ETC (7) and (8).

Proof. When $t \in [t_\iota, t_{\iota+1}), \iota = 1, 2, \cdots$,

$$\frac{\mathrm{d}|\mathcal{E}_{1s}(t)|}{\mathrm{d}t} \leq \frac{\mathrm{d}|\mathcal{U}_{1s}(t)|}{\mathrm{d}t} \leq [\rho_s + (2\omega-1)\sigma_s\chi_s^{2\omega-2}(t)]|\frac{\mathrm{d}\chi_s(t)}{\mathrm{d}t}|. \tag{18}$$

From systems (6), one has

$$\frac{\mathrm{d}\chi_s(t)}{\mathrm{d}t} \leq J_s^{min}|\chi_s(t)| + \sum_{s=1}^{\hbar} a_{sz}^{max}M + \sum_{s=1}^{\hbar} b_{sz}^{max}M + \sum_{s=1}^{\hbar} c_{sz}^{max}\sigma_z M + |\breve{u}_{1s}(t)|. \tag{19}$$

Due to

$$\frac{\mathrm{d}V(t)}{\mathrm{d}t} < 0,$$

thus,

$$|\chi_s(t)| \leq V(0),$$

then

$$\begin{aligned}\frac{\mathrm{d}\chi_s(t)}{\mathrm{d}t} &\leq J_s^{min}V(0) + \sum_{s=1}^{\hbar} a_{sz}^{max}M + \sum_{s=1}^{\hbar} b_{sz}^{max}M + \sum_{s=1}^{\hbar} c_{sz}^{max}\sigma_z M + |\breve{u}_{1s}(t)| \\ &= F_s(t_\iota) \\ &> 0. \end{aligned} \tag{20}$$

Let

$$\Psi_s = \max_{t\in[t_\iota,t_{\iota+1})}[\rho_s + (2\omega-1)\sigma_s\chi_s^{2\omega-2}(t)],$$

and by using (17), one gets

$$\frac{\mathrm{d}|\mathcal{E}_{1s}(t)|}{\mathrm{d}t} \leq \Psi_s F_s(t_\iota). \tag{21}$$

Because $|\mathcal{E}_{1s}(t_\iota)| = 0$, then

$$|\mathcal{E}_{1s}(t)| \leq \int_{t_\iota}^{t} \Psi_s F_s(t_\iota)\mathrm{d}s = \Psi_s F_s(t_\iota)(t-t_\iota). \tag{22}$$

From ETC (8), one derives

$$\begin{aligned} |\mathcal{E}_{1s}(t_{\iota+1})| &\geq \varsigma_s|\chi_s(t_{\iota+1})| + \alpha_s\sigma_s|\chi_s^{2\omega-1}(t_{\iota+1})| + \gamma_s(1-\vartheta_s)^{t_{\iota+1}} \\ &\geq \gamma_s(1-\vartheta_s)^{t_{\iota+1}} \\ &> 0. \end{aligned} \tag{23}$$

From (22) and (23), one has

$$t_{\iota+1} - t_\iota \geq \frac{\gamma_s(1-\vartheta_s)^{t_{\iota+1}}}{\Psi_s F_s(t_\iota)} > 0. \tag{24}$$

The proof is finished. □

The subsequent discussion is the exceptional case of the FTS model for system (3) under $r_z(t) = 0$.

If $r_z(t) = 0$, $\mathfrak{I}_s(0) = 0$, and (1) appears to have prolonged oscillation or chaotic behaviors, the stabilization model on SDSNNs (3) is

$$\frac{\mathrm{d}\chi_s(t)}{\mathrm{d}t} = -\jmath_s(\chi_s(t))\chi_s(t) + \sum_{z=1}^{\hbar} a_{sz}(\chi_s(t))\mathfrak{I}_z(\chi_z(t)) + \sum_{z=1}^{\hbar} b_{sz}(\chi_s(t))\mathfrak{I}_z(\chi_z(t-\tau_z(t))) + \mathfrak{U}_{1s}(t),\ t\geq 0, s\in\mathcal{W}, \tag{25}$$

in which $\mathfrak{U}_{1s}(t)$ $(s \in \mathcal{W})$ is

$$\mathfrak{U}_{1s}(t) = -\tilde{\rho}_s\chi_s(t_\iota) - \tilde{\sigma}_s[\chi^2(t_\iota)]^{\tilde{\omega}-1}\chi_s(t_\iota) - \tilde{\kappa}_s\phi_s(t_\iota), \quad t\in[t_\iota, t_{\iota+1}), \iota = 1, 2, \cdots, \tag{26}$$

where $\tilde{\rho}_s, \tilde{\sigma}_s, \tilde{\kappa}_s$ are all positive constants,

$$\tilde{\omega} = \tilde{\lambda} + sign(V(t)-1), \quad 1 < \tilde{\lambda} < 2.$$

For $t \in [t_\iota, t_{\iota+1})$, let

$$\mathfrak{U}_{1s}^*(t) = -\tilde{\rho}_s\chi_s(t) - \tilde{\sigma}_s[\chi^2(t)]^{\tilde{\omega}-1}\chi_s(t) - \tilde{\kappa}_s\phi_s(t).$$

The measure error is

$$\mathbb{E}_{1s}(t) = \mathfrak{U}_{1s}^*(t) - \mathfrak{U}_{1s}(t),$$

and event-triggering is

$$t_{\iota+1} = \{t|t > t_\iota, |\mathbb{E}_{1s}(t)| \geq \tilde{\varsigma}_s|\chi_s(t)| + \tilde{\alpha}_s\tilde{\sigma}_s|\chi_s^{2\tilde{\omega}-1}(t)| + \tilde{\gamma}_s(1-\tilde{\vartheta}_s)^t\}, \tag{27}$$

where $\tilde{\alpha}_s, \tilde{\vartheta}_s \in (0,1), \tilde{\varsigma}_s, \tilde{\gamma}_s > 0$, and t_ι ($\iota = 0,1,2,\cdots, s \in \mathbb{N}$) is the ι th triggering instant.

Let

$$\tilde{\kappa}_s \geq \sum_{z=1}^{\hbar} a_{sz}^{max} M + \sum_{z=1}^{\hbar} b_{sz}^{max} M + \tilde{\gamma}_s. \tag{28}$$
$$\tilde{\zeta}_s = 2(\jmath_s^{min} + \tilde{\rho}_s - \tilde{\varsigma}_s), \quad s \in \mathcal{W}.$$

The following Corollary 1 of Theorem 1 can be derived from above.

Corollary 1. Under Assumption 1, Lemma 2, ETC (26) and (27), if (28) and $\tilde{\zeta}_s > 0, r_z(t) = 0$ ($s, z \in \mathcal{W}$) hold, then SDSNNs (3) achieve FTS, and the settling-time is T_{max}.

3.2. *PTS of SDSNNs (3)*

In this part, we build some results on PTS about SDSNNs (3) first, then the following controller is proposed:

$$\begin{aligned}\breve{u}_{2s}(t) = &-[\frac{T_{max}}{T_p}(\rho_s + \eta_s) - \eta_s]\chi_s(t_\iota) - [\frac{T_{max}}{T_p}(\sigma_s - \alpha_s\sigma_s) + \alpha_s\sigma_s][\chi_s^2(t_\iota)]^{\omega-1}\chi_s(t_\iota)\\ &- \kappa_s\phi_s(t_\iota), \quad t \in [t_\iota, t_{\iota+1}), \ \iota = 1,2,\cdots.\end{aligned} \tag{29}$$

Here, $\rho_s, \sigma_s, \kappa_s$ are all positive constants,

$$\omega = \lambda + sign(V(t) - 1)$$

for $t \in [t_\iota, t_{\iota+1})$, $1 < \lambda < 2$ and $\eta_s = \jmath_s^{min} - \varsigma_s$, T_p is preassigned-time and T_{max} is defined in Theorem 2.

Let

$$\breve{\mathcal{U}}_{2s}(t) = -[\frac{T_{max}}{T_p}(\rho_s + \eta_s) - \eta_s]\chi_s(t) - [\frac{T_{max}}{T_p}(\sigma_s - \alpha_s\sigma_s) + \alpha_s\sigma_s][\chi_s^2(t)]^{\omega-1}\chi_s(t) - \kappa_s\phi_s(t). \tag{30}$$

The measure error is

$$\mathcal{E}_{2s}(t) = \breve{\mathcal{U}}_{2s}(t) - \breve{u}_{2s}(t).$$

The event-triggering is

$$t_{\iota+1} = \{t | t > t_\iota, |\mathcal{E}_{2s}(t)| \geq \varsigma_s|\chi_s(t)| + \alpha_s\sigma_s|\chi_s^{2\omega-1}(t)| + \gamma_s(1 - \vartheta_s)^t\}, \tag{31}$$

where $\alpha_s, \vartheta_s \in (0,1), \varsigma_s, \gamma_s > 0$, and t_ι ($\iota = 0,1,2,\cdots, s \in \mathbb{N}$) is the ιth triggering instant.

Let

$$\kappa_s \geq \sum_{z=1}^{\hbar} a_{sz}^{max} M + \sum_{z=1}^{\hbar} b_{sz}^{max} M + \sum_{z=1}^{\hbar} c_{sz}^{max} M r_z + \gamma_s, \tag{32}$$
$$\eta_s = \jmath_s^{min} - \varsigma_s, \tag{33}$$
$$\zeta_s = 2(\jmath_s^{min} + \rho_s - \varsigma_s), \quad s \in \mathcal{W}, \tag{34}$$

The main results of this subsection are presented as follows.

Remark 4. Differing from studies on asymptotic stability in [5, 25, 31] and finite-time stability in [14, 15, 27, 28], the fixed/preassigned-time stability performance ensures that the settling time is independent of initial conditions. In [18, 19, 21–24, 30, 35], the control methods commonly used are feedback control, requiring continuous system control. However, the ETC strategy adopted in this paper, ETC (7), (8), (30) and (31), can reduce the frequency of control operations, thereby decreasing system energy consumption.

Theorem 3. Under Assumption 1, Lemma 3, and ETC (30) and (31), if (32), (33), and $\zeta_s > 0$ ($s \in \mathcal{W}$) hold, SDSNNs (3) get PTS, the settling-time is T_{max}, and the preassigned-time is T_p.

Proof. Introduce a Lyapunov function

$$V(t) = \sum_{s=1}^{\hbar} \chi_s^2(t). \tag{35}$$

Similar to the proof of Theorem 1, one has

$$\begin{aligned}
\frac{\mathrm{d}V(t)}{\mathrm{d}t} \leq & -2\sum_{s=1}^{\hbar} J_s^{min}\chi_s^2(t) + 2\sum_{s=1}^{\hbar}\sum_{z=1}^{\hbar} a_{sz}^{max} M|\chi_s(t)| + 2\sum_{s=1}^{\hbar}\sum_{z=1}^{\hbar} b_{sz}^{max} M|\chi_s(t)| \\
& + 2\sum_{s=1}^{\hbar}\sum_{z=1}^{\hbar} c_{sz}^{max} r_z M|\chi_s(t)| + 2\sum_{s=1}^{\hbar} \phi_s(t)\chi_s(t)(\check{\mathcal{U}}_{2s}(t) - \mathcal{E}_{2s}(t)) \\
\leq & -2\sum_{s=1}^{\hbar} J_s^{min}\chi_s^2(t) + 2\sum_{s=1}^{\hbar}\sum_{z=1}^{\hbar} a_{sz}^{max} M|\chi_s(t)| + 2\sum_{s=1}^{\hbar}\sum_{z=1}^{\hbar} b_{sz}^{max} M|\chi_s(t)| \\
& + 2\sum_{s=1}^{\hbar}\sum_{z=1}^{\hbar} c_{sz}^{max} r_z M|\chi_s(t)| + 2\sum_{s=1}^{\hbar} \phi_s(t)\chi_s(t)\{-[\frac{T_{max}}{T_p}(\rho_s + \eta_s) - \eta_s]\chi_s(t) \\
& - [\frac{T_{max}}{T_p}(\sigma_s - \alpha_s\sigma_s) + \alpha_s\sigma_s][\chi^2(t)]^{\omega-1}\chi_s(t) - \kappa_s\phi_s(t)\} \\
\leq & -2\sum_{s=1}^{\hbar}[J_s^{min} - \varsigma_s - \eta_s + \frac{T_{max}}{T_p}(\rho_s + \eta_s)]\chi_s^2(t) \\
& + 2\sum_{s=1}^{\hbar}|\chi_s(t)|[\sum_{z=1}^{\hbar} a_{sz}^{max} M + \sum_{z=1}^{\hbar} b_{sz}^{max} M + \sum_{z=1}^{\hbar} c_{sz}^{max} r_z M - \kappa_s + \gamma_s] \\
& - 2\sum_{s=1}^{\hbar}[\chi_s^2(t)]^{\omega}[\frac{T_{max}}{T_p}(\sigma_s - \alpha_s\sigma_s) + \alpha_s\sigma_s - \alpha_s\sigma_s] \\
& + 2\sum_{s=1}^{\hbar}|\chi_s(t)|[|\mathcal{E}_{2s}(t)| - \varsigma_s|\chi_s(t)| - \alpha_s\sigma_s|\chi_s^{2\omega-1}(t)| - \gamma_s(1-\vartheta_s)^t] \\
\leq & \sum_{z=1}^{\hbar} \frac{T_{max}}{T_p}\{-\zeta_s\chi_s^2(t) - 2(1-\alpha_s)\sigma_s[\chi_s^2(t)]^{\omega}\}.
\end{aligned} \tag{36}$$

By using conditions (31)–(34), one knows

$$\frac{\mathrm{d}V(t)}{\mathrm{d}t} \leq \sum_{s=1}^{\hbar} \frac{T_{max}}{T_p}\{-\zeta_s\chi_s^2(t) - 2(1-\alpha_s)\sigma_s[\chi_s^2(t)]^{\omega}\}. \tag{37}$$

Utilizing Lemma 1 in [36], one can derive:

(1) If $V(t) \in (0, 1)$,

$$\begin{aligned} -\sum_{s=1}^{\hbar} 2(1-\alpha_s)\sigma_s[\chi_s^2(t)]^{\omega} &\leq -\Re_1 \sum_{s=1}^{\hbar}[\chi_s^2(t)]^{\omega} \\ &= -\Re_1 V^{\omega}(t), \end{aligned} \tag{38}$$

in which

$$\Re_1 = min_{s\in\mathcal{W}}\{2(1-\alpha_s)\sigma_s\}.$$

(2) If $V(t) \geq 1$,

$$\begin{aligned} -\sum_{s=1}^{\hbar} 2(1-\alpha_s)\sigma_s[\chi_s^2(t)]^{\omega} &\leq -\Re_2 \sum_{s=1}^{\hbar}[\chi_s^2(t)]^{\omega} \\ &= -\Re_2 V^{\omega}(t), \end{aligned} \tag{39}$$

where $\Re_2 = \Re_1\hbar^{-\lambda}$. From (36)–(39), one obtains

$$\frac{\mathrm{d}V(y(t))}{\mathrm{d}t} \leq \frac{T_{max}}{T_p}[-\zeta V(y(t)) - \Re V^{\omega}(y(t))], \tag{40}$$

where

$$\Re = min\{\Re_1, \Re_2\}, \quad \zeta = min_{s\in\mathcal{W}}\{\zeta_s\}, \quad \zeta < \{\Re_1, \Re_2\}.$$

From Definition 2 and Lemma 3, we get SDSNNs (3) to achieve PTS at the preassigned-time T_p. The proof is finished. □

Remark 5. The system (6) can also avoid Zeno-behavior under ETC (30) and (31) and its proof process is the same as Theorem 2.

The subsequent discussion is the exceptional case of the PTS model for system (3) under $r_z(t) = 0$.

If $r_z(t) = 0$, $\Im_s(0) = 0$, and (1) appears to have prolonged oscillation or chaotic behaviors, the stabilization model on SDSNNs (3) is

$$\frac{\mathrm{d}\chi_s(t)}{\mathrm{d}t} = -\jmath_s(\chi_s(t))\chi_s(t) + \sum_{z=1}^{\hbar} a_{sz}(\chi_s(t))\Im_z(\chi_z(t)) + \sum_{z=1}^{\hbar} b_{sz}(\chi_s(t))\Im_z(\chi_z(t-\tau_z(t))) + \mathfrak{U}_{2s}(t),\ t \geq 0, s \in \mathcal{W}, \tag{41}$$

in which $\mathfrak{U}_{2s}(t)$ $(s \in \mathcal{W})$ is

$$\mathfrak{U}_{2s}(t) = -[\frac{T_{max}}{T_p}(\tilde{\rho}_s + \tilde{\eta}_s) - \tilde{\eta}_s]\chi_s(t_\iota) - [\frac{T_{max}}{T_p}(\tilde{\sigma}_s - \tilde{\alpha}_s\tilde{\sigma}_s) + \tilde{\alpha}_s\tilde{\sigma}_s][\chi^2(t_\iota)]^{\tilde{\omega}-1}\chi_s(t_\iota) - \tilde{\kappa}_s\phi_s(t_\iota), \tag{42}$$

where $t \in [t_\iota, t_{\iota+1}), \iota = 1, 2, \cdots$. Here, $\tilde{\rho}_s, \tilde{\sigma}_s, \tilde{\kappa}_s$ are all positive constants,

$$\tilde{\omega} = \tilde{\lambda} + sign(V(t) - 1)$$

for $t \in [t_\iota, t_{\iota+1})$ and $1 < \tilde{\lambda} < 2$.

Let

$$\mathfrak{U}_{2s}^*(t) = -[\frac{T_{max}}{T_p}(\tilde{\rho}_s + \tilde{\eta}_s) - \tilde{\eta}_s]\chi_s(t) - [\frac{T_{max}}{T_p}(\tilde{\sigma}_s - \tilde{\alpha}_s\tilde{\sigma}_s) + \tilde{\alpha}_s\tilde{\sigma}_s][\chi^2(t)]^{\tilde{\omega}-1}\chi_s(t) - \tilde{\kappa}_s\phi_s(t). \tag{43}$$

The measure error is

$$\mathbb{E}_{2s}(t) = \mathfrak{U}_{2s}^*(t) - \mathfrak{U}_{2s}(t),$$

and event-triggering is

$$t_{\iota+1} = \{t | t > t_\iota, |\mathbb{E}_{2s}(t)| \geq \tilde{\varsigma}_s|\chi_s(t)| + \tilde{\alpha}_s\tilde{\sigma}_s|\chi_s^{2\tilde{\omega}-1}(t)| + \tilde{\gamma}_s(1 - \tilde{\vartheta}_s)^t\}, \tag{44}$$

where $\tilde{\alpha}_s, \tilde{\vartheta}_s \in (0, 1), \tilde{\varsigma}_s, \tilde{\gamma}_s > 0$, and t_ι ($\iota = 0, 1, 2, \cdots, s \in \mathbb{N}$) is the ι th triggering instant.

Let

$$\tilde{\kappa}_s \geq \sum_{z=1}^{\hbar} a_{sz}^{max} M + \sum_{z=1}^{\hbar} b_{sz}^{max} M + \tilde{\gamma}_s, \tag{45}$$

$$\tilde{\eta}_s = J_s^{min} - \tilde{\varsigma}_s, \tag{46}$$

and

$$\tilde{\zeta}_s = 2(J_s^{min} + \tilde{\rho}_s - \tilde{\varsigma}_s), \quad s \in \mathcal{W}.$$

The following Corollary 2 of Theorem 3 can be derived from the above.

Corollary 2. Under Assumption 1, Lemma 3, and ETC (43) and (44), if (45), (46), $\zeta_s > 0$, and $r_z(t) = 0$ ($s, z \in \mathcal{W}$) hold, SDSNNs (3) achieve PTS and the preassigned-time is T_p.

Remark 6. In recent years, there have been several studies on finite and FTS with state switching (see [14, 15, 18, 19]). Unfortunately, these studies did not consider PTS results and lacked flexibility in the controllers, leading to higher power consumption for the systems. Additionally, [18, 20] only considered systems with time-varying delays and could not adapt to the multiple delays present in some complex systems. This paper optimizes the state switching mechanism, introduces an ETC scheme, and enriches the existing stability results for this model; therefore, the SDSNNs presented in this work exhibit greater flexibility and applicability.

Remark 7. The control mechanism and state switching mechanism used in this study can be further expanded through the integration with various models, allowing for more complex research. With its performance advantages, they can also be extended to fields such as financial prediction, medical diagnosis, computer vision, etc., thus possessing the ability for broader dissemination and application.

4. Numerical example

Now, a numerical simulation example is used to demonstrate the FTS and PTS results separately.

Consider the following 2-neuron SDSNNs as the FTS system

$$\frac{\mathrm{d}\chi_s(t)}{\mathrm{d}t} = -\jmath_s(\chi_s(t))\chi_s(t) + \sum_{z=1}^{2} a_{sz}(\chi_s(t))\mathfrak{I}_z(\chi_z(t)) + \sum_{z=1}^{2} b_{sz}(\chi_s(t))\mathfrak{I}_z(\chi_z(t-\tau_z(t))) + \sum_{z=1}^{2} c_{sz}(\chi_s(t))\int_{t-r_z(t)}^{t} \mathfrak{I}_z(\chi_z(\upsilon))\mathrm{d}\upsilon + \breve{u}_{1s}(t), \quad t \geq 0, s \in \mathcal{W}, \tag{47}$$

where we take the activation function as

$$f_1(\cdot) = f_2(\cdot) = sin(\cdot),$$

the time-varying delay as

$$\tau_z(t) = 0.4 - 0.1 sin(t),$$

and the distributed delay as

$$r_z(t) = 0.65 - 0.15 sin(t), \quad z = 1, 2.$$

The initial conditon of the master system is

$$\chi_1(\upsilon) = -2, \ \ \chi_2(\upsilon) = 3.5, \ \ \upsilon \in (-0.8, 0].$$

Without ETC, the oscillation state $\chi_1(t), \chi_2(t)$ is shown in Figure 1.

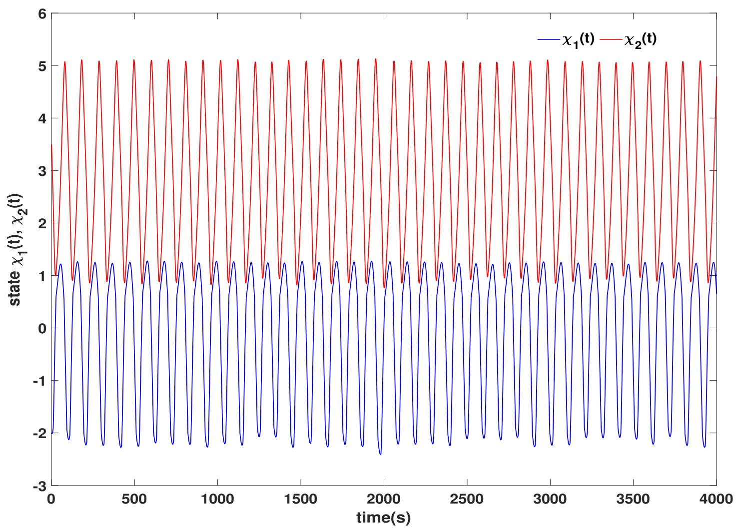

Figure 1. State trajectory diagram for (47) and (48) without ETC.

On the basis of satisfying the constraints of parameters in (7) and (8), we randomly select, $\rho_1 = \rho_2 = 27, \varsigma_1 = 28.85, \varsigma_2 = 29,6, \gamma_1 = \gamma_2 = 0.1, \alpha_1 = \alpha_2 = 0.97, \sigma_1 = \sigma_2 = 4, \vartheta_1 = \vartheta_2 = 0.8, \lambda = 1.1$, then, by using (9) and (10), we get $\kappa_1 = 16.74, \kappa_2 = 17.22, \zeta = 0.1$. The values of $\mathfrak{R}_1$ and $\mathfrak{R}_2$ obtained from (15) and (16) can be easily calculated to yield $\mathfrak{R}_1 = 0.24, \mathfrak{R}_2 = 0.112$.

According to Lemma 2, $T_{max} = 9.671$ is calculated, and Figure 2 demonstrates that the system (47) can reach stability within T_{max}.

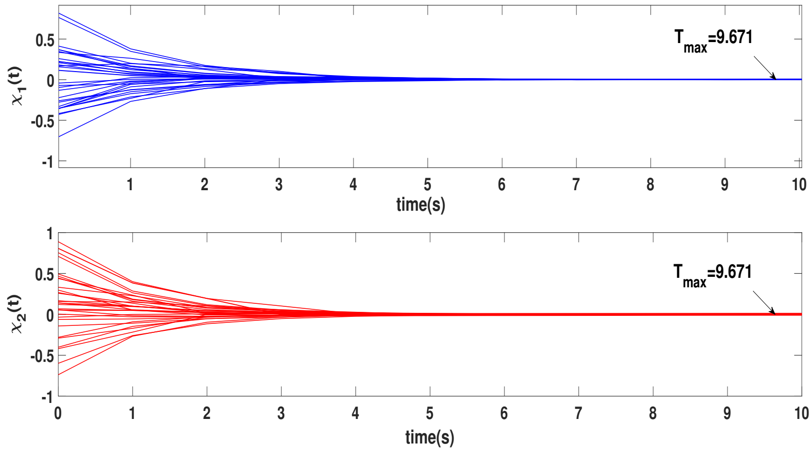

Figure 2. State trajectory of FTS for $\chi_1(t)$ and $\chi_2(t)$ under ETC (7) and (8).

Combining the notation section in the introduction and (2), the master system parameters are specified as follows:

$$j_1^*(t) = 1.1, \quad j_1^{**}(t) = 1.2, \quad j_2^*(t) = -0.21, \quad j_2^{**}(t) = -0.2,$$

$$a_{11}^* = 0.01, \quad a_{11}^{**} = 0.2, \quad a_{12}^* = 6, \quad a_{12}^{**} = 5.8, \quad a_{21}^* = 5.8, \quad a_{21}^{**} = 5.5, \quad a_{22}^* = -2, \quad a_{22}^{**} = -1,$$

$$b_{11}^* = -3, \quad b_{11}^{**} = -3, \quad b_{12}^* = 4, \quad b_{12}^{**} = 4, \quad b_{21}^* = 5.9, \quad b_{21}^{**} = 5.9, \quad b_{22}^* = 1.5, \quad b_{22}^{**} = 1.5,$$

$$c_{11}^* = -4.1, \quad c_{11}^{**} = -3.9, \quad c_{12}^* = -0.2, vc_{12}^{**} = -0.15, \quad c_{21}^* = -1.1, \quad c_{21}^{**} = -1.2, \quad c_{22}^* = 1.2, \quad c_{22}^{**} = 1.19.$$

By utilizing Theorem 1 under the conditions of ETC (7) and (8), we randomly selected 30 starting values. $\chi_1(t), \chi_2(t)$ of SDSNNs (47) are shown in Figure 2 and they clearly indicate that FTS is achieved independently of the system's initial values, and the 30 control signals corresponding $\breve{u}_{1s}(t)$ to Figure 2 are shown in Figure 3. The time intervals between events of ETC are shown in Figure 4; therefore, we can observe that the controller only performs control operations when specific events occur, thereby reducing computational and communication overhead. From Figures 1–4, it can be concluded that the ETC (7) and (8) proposed in this paper are very effective in achieving the FTS in SDSNNs (47).

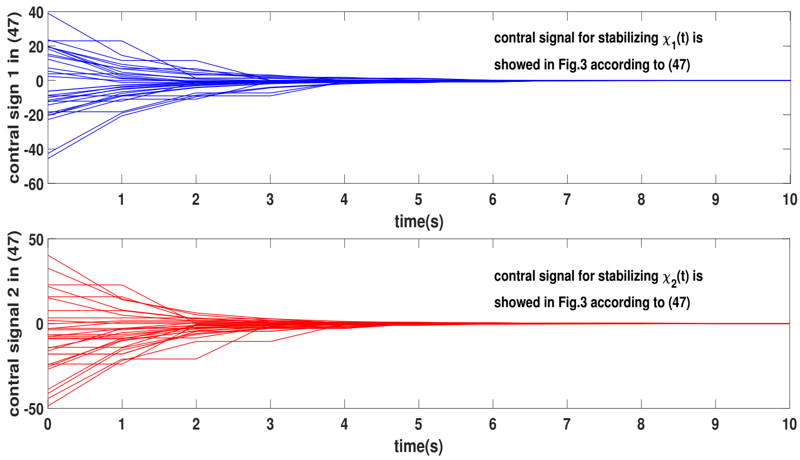

Figure 3. Control signals for stabilizing states $\chi_1(t)$ and $\chi_2(t)$ in Figure 2.

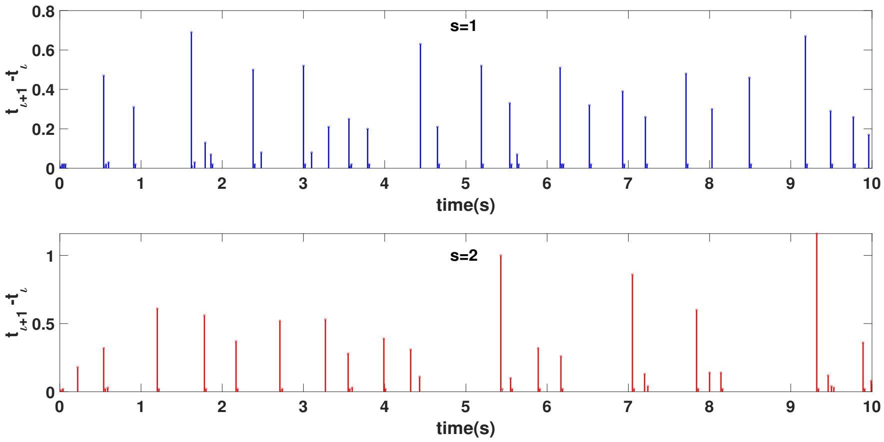

Figure 4. ETC (7) and (8) transmission time interval.

Consider a 2-neuron SDSNNs as the PTS system

$$\frac{\mathrm{d}\chi_s(t)}{\mathrm{d}t} = -\jmath_s(\chi_s(t))\chi_s(t) + \sum_{z=1}^{2} a_{sz}(\chi_s(t))\Im_z(\chi_z(t)) + \sum_{z=1}^{2} b_{sz}(\chi_s(t))\Im_z(\chi_z(t-\tau_z(t)))$$
$$+ \sum_{z=1}^{2} c_{sz}(\chi_s(t)) \int_{t-r_z(t)}^{t} \Im_z(\chi_z(\upsilon))\mathrm{d}\upsilon + \breve{u}_{2s}(t), \quad t \geq 0, s \in \mathcal{W}. \tag{48}$$

From (48), we keep all other parameters the same as those shown in the above FTS, and additionally set prescribed-time $T_p = 9 < T_{max} = 9.671$, which does not depend on any master system and the initial values. Under the influence of the preassigned-time $T_p = 9$, the master system can achieve PTS by using the controller described in (48).

By utilizing Theorem 3 under the conditions of ETC (30) and (31), we randomly selected 30 starting values and state $\chi_1(t)$, $\chi_2(t)$ of SDSNNs (48), as shown in Figure 5. The 30 control signals corresponding $\breve{u}_{2s}(t)$ to Figure 5 are shown in Figure 6, and the time intervals between events of ETC are presented in Figure 7. From Figures 1 and 5–7, it can be concluded that the ETC (30) and (31) proposed in this paper are very effective in achieving the PTS in SDSNNs (48).

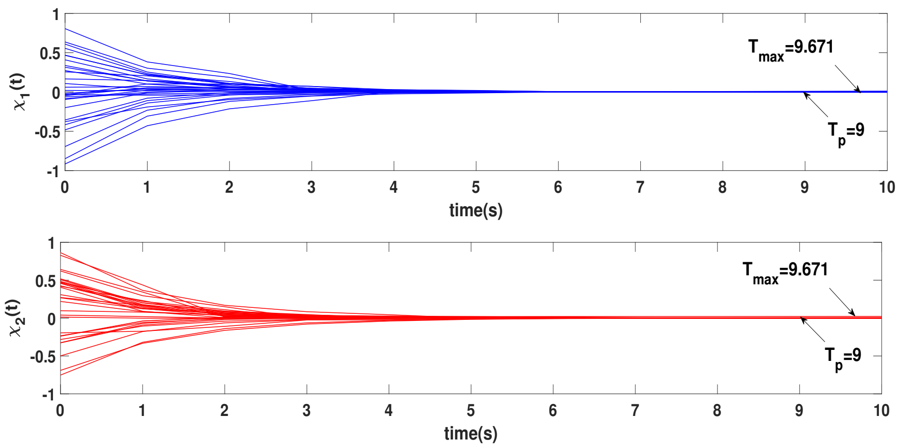

Figure 5. State trajectory of PTS for $\chi_1(t)$ and $\chi_2(t)$ under ETC (30) and (31).

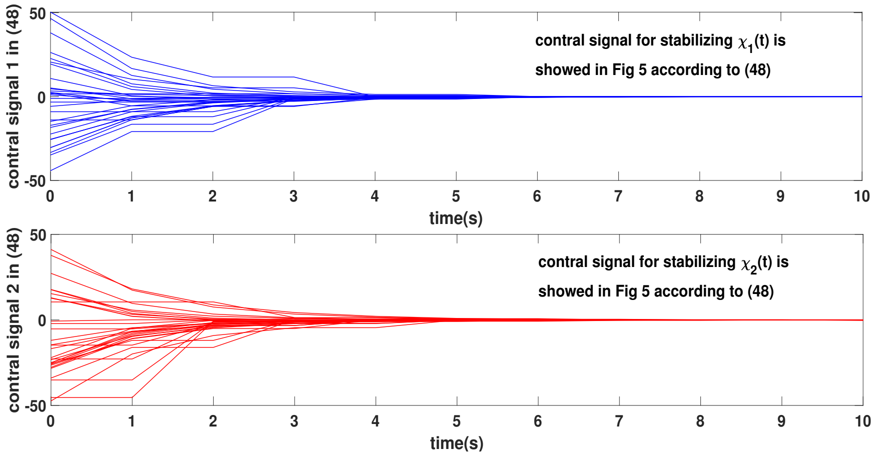

Figure 6. Control signals for stabilizing states $\chi_1(t)$ and $\chi_2(t)$ in Figure 5.

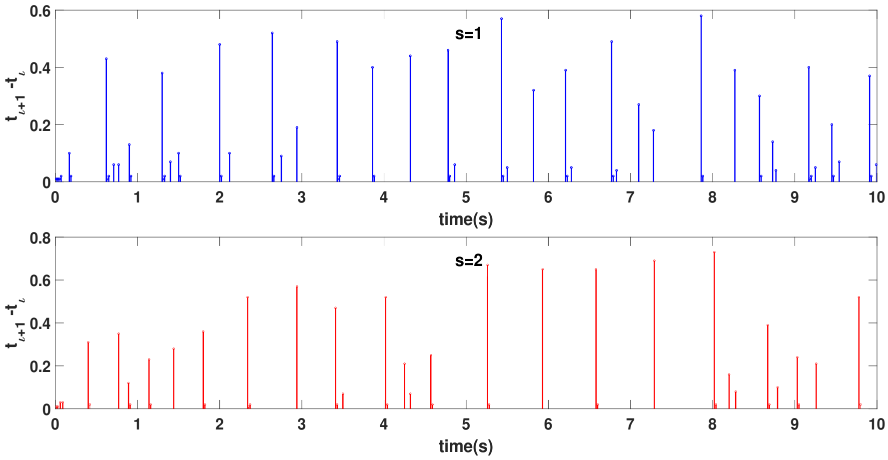

Figure 7. ETC (30) and (31) transmission time interval.

5. Conclusions

This paper considered a kind of SDSNNs architecture that incorporates mixed time delays. The state switching mechanism used here is a complex switching with derivatives, which facilitates a faster adjustment of network parameters and speeds up convergence. Furthermore, an ETC strategy is employed to effectively reduce the frequency of control operations, thereby reducing power consumption. The main system achieves FTS and PTS results, allowing the system's settling time to be free from initial condition control and enriching the stability results of this model.

As we know, the necessity of studying the synchronicity of neural networks lies in gaining a deeper understanding of the coordination and interactions between neurons in the brain, which is crucial for cognitive functions such as information processing, learning, and memory. Additionally, complex numbers and quaternions have significant applications in information processing within neural systems. Therefore, we plan to discuss the synchronization issues of SDSNNs in future works and expand our research to address problems related to complex numbers and quaternions.

Use of AI tools declaration

The authors declare they have not used Artificial Intelligence (AI) tools in the creation of this article.

Acknowledgments

This work is supported by the National Science Foundation of China under Grant No. 61976228.

Conflict of interest

All authors declare no conflicts of interest in this paper.

References

1. J. Cheng, X. Jiang, H. Zhou, J. Dong, Research progress and challenges of photoelectric intelligent computing, *China Laser*, **49** (2022), 327–339.
2. L. Chua, Memristor-the missing circuit element, *IEEE Trans. Circuit Theory*, **18** (1971), 507–519. https://doi.org/10.1109/TCT.1971.1083337
3. D. B. Strukov, G. S. Snider, D. R. Stewart, R. S. Williams, The missing memristor found, *Nature*, **453** (2008), 80–83.
4. G. Zhang, Z. Zeng, D. Ning, Novel results on synchronization for a class of switched inertial neural networks with distributed delays, *Inf. Sci.*, **511** (2020), 114–126. https://doi.org/10.1016/j.ins.2019.09.048
5. G. Zhang, J. Cao, A. Kashkynbayev, Further results on fixed/preassigned-time projective lag synchronization control of hybrid inertial neural networks with time delays, *J. Franklin Inst.*, **360** (2023), 9950–9973. https://doi.org/10.1016/j.jfranklin.2023.07.040
6. G. Milano, M. Agliuzza, N. de Leo, C. Ricciardi, Speech recognition through physical reservoir computing with neuromorphic nanowire networks, *2022 International Joint Conference on Neural Networks (IJCNN)*, 2022. https://doi.org/10.1109/IJCNN55064.2022.9892078
7. J. X. Zhang, T. Yang, T. Chai, Neural network control of underactuated surface vehicles with prescribed trajectory tracking performance, *IEEE Trans. Neural Networks Learn. Syst.*, 2022. https://doi.org/10.1109/TNNLS.2022.3223666
8. G. Qin, A. Lin, J. Cheng, M. Hu, I. Katib, Protocol-based fault detection filtering for memristive neural networks with dynamic quantization, *J. Franklin Inst.*, **360** (2023), 13395–13413. https://doi.org/10.1016/j.jfranklin.2023.10.019
9. J. X. Zhang, T. Chai, Proportional-integral funnel control of unknown lower-triangular nonlinear systems, *IEEE Trans. Autom. Control*, 2023. https://doi.org/10.1109/TAC.2023.3330900
10. C. Xu, W. Ou, Y. Pang, Q. Cui, M. U. Rahman, M. Farman, et al., Hopf bifurcation control of a fractional-order delayed turbidostat model via a novel extended hybrid controller, *MATCH Commun. Math. Comput. Chem.*, **91** (2024), 367–413. https://doi.org/10.46793/match.91-2.367X
11. C. Xu, Z. Liu, P. Li, J. Yan, L. Yao, Bifurcation mechanism for fractional-order three-triangle multi-delayed neural networks, *Neural Process. Lett.*, **55** (2023), 6125–6151. https://doi.org/10.1007/s11063-022-11130-y

12. C. Xu, Q. Cui, Z. Liu, Y. Pan, X. Cui, W. Ou, et al., Extended hybrid controller design of bifurcation in a delayed chemostat model, *MATCH Commun. Math. Comput. Chem.*, **90** (2023), 609–648. https://doi.org/10.46793/match.90-3.609X
13. H. Guo, J. Han, G. Zhang, Hopf bifurcation and control for the bioeconomic predator-prey model with square root functional response and nonlinear prey harvesting, *Mathematics*, **11** (2023), 4958. https://doi.org/10.3390/math11244958
14. M. J. Mirzaei, E. Aslmostafa, M. Asadollahi, M. A. Badamchizadeh, Robust adaptive finite-time stabilization control for a class of nonlinear switched systems based on finite-time disturbance observer, *J. Franklin Inst.*, **358** (2021), 3332–3352. https://doi.org/10.1016/j.jfranklin.2021.02.010
15. N. Xu, Y. Chen, A. Xue, G. Zong, Finite-time stabilization of continuous-time switched positive delayed systems, *J. Franklin Inst.*, **359** (2022), 255–271. https://doi.org/10.1016/j.jfranklin.2021.04.022
16. S. Kanakalakshmi, R. Sakthivel, S. Karthick, A. Leelamani, A. Parivallal, Finite-time decentralized event-triggering non-fragile control for fuzzy neural networks with cyber-attack and energy constraints, *Eur. J. Control*, **57** (2021), 135–146, https://doi.org/10.1016/j.ejcon.2020.05.001
17. M. M. Silva, X. Wang, F. E. Alsaadi, Y. Shen, Fixed-time synchronization and parameter identification of coupled neural networks, *Neural Networks*, **77** (2016), 40–47.
18. X. Hu, L. Wang, C. K. Zhang, X. Wan, Y. He, Fixed-time stabilization of discontinuous spatiotemporal neural networks with time-varying coefficients via aperiodically switching control, *Sci. China Inf. Sci.*, **66** (2023), 152204. https://doi.org/10.1007/s11432-022-3633-9
19. Y. Bao, Y. Zhang, B. Zhang, Resilient fixed-time stabilization of switched neural networks subjected to impulsive deception attacks, *Neural Networks*, **163** (2023), 312–326, https://doi.org/10.1016/j.neunet.2023.04.003
20. G. Zhang, Novel results on event-triggered-based fixed-time synchronization and stabilization of discontinuous neural networks with distributed delays, *Franklin Open*, **4** (2023), 100032. https://doi.org/10.1016/j.fraope.2023.100032
21. Y. Zhang, F. Kong, L. Wang, C. Hu, Fixed-time stabilization of generalized leakage-delayed neural networks with discontinuous disturbances via mixed-delay-product-type LKF, *Eur. J. Control*, **71** (2023), 100793. https://doi.org/10.1016/j.ejcon.2023.100793
22. F. Tan, L. Zhou, J. Lu, H. Zhang, Fixed-time synchronization in multilayer networks with delay cohen–grossberg neural subnets via adaptive quantitative control, *Asian J. Control*, **26** (2024), 446–455. https://doi.org/10.1002/asjc.3217
23. Q. Gan, L. Li, J. Yang, Y. Qin, M. Meng, Improved results on fixed-/preassigned-time synchronization for memristive complex-valued neural networks, *IEEE Trans. Neural Networks Learn. Syst.*, **33** (2021), 5542–5556. https://doi.org/10.1109/TNNLS.2021.3070966
24. H. Li, C. Hu, G. Zhang, J. Hu, L. Wang, Fixed-/preassigned-time stabilization of delayed memristive neural networks, *Inf. Sci.*, **610** (2022), 624–636. https://doi.org/10.1016/j.ins.2022.08.011
25. Z. Yan, X. Huang, J. Cao, Variable-sampling-period dependent global stabilization of delayed memristive neural networks based on refined switching event-triggered control, *Sci. China Inf. Sci.*, **63** (2020), 212201. https://doi.org/10.1007/s11432-019-2664-7

26. R. Zhao, Z. Zuo, Y. Wang, Event-triggered control for networked switched systems with quantization, *IEEE Trans. Syst. Man Cybern.*, **52** (2022), 6120–6128. https://doi.org/10.1109/TSMC.2021.3139386
27. J. Ping, S. Zhu, M. Shi, S. Wu, M. Shen, X. Liu, et al., Event-triggered finite-time synchronization control for quaternion-valued memristive neural networks by an non-decomposition method, *IEEE Trans. Network Sci. Eng.*, **10** (2023), 3609–3619. https://doi.org/10.1109/TNSE.2023.3268101
28. J. Ping, S. Zhu, X. Liu, Finite/fixed-time synchronization of memristive neural networks via event-triggered control, *Knowl. Based Syst.*, **258** (2022), 110013. https://doi.org/10.1016/j.knosys.2022.110013
29. Y. Zhou, H. Zhang, Z. Zeng, Synchronization of memristive neural networks with unknown parameters via event-triggered adaptive control, *Neural Networks*, **139** (2021), 255–264. https://doi.org/10.1016/j.neunet.2021.02.029
30. N. Li, X. Wu, J. Feng, J. Lü, Fixed-time synchronization of complex dynamical networks: a novel and economical mechanism, *IEEE Trans. Cybern.*, **52** (2022), 4430–4440. https://doi.org/10.1109/TCYB.2020.3026996
31. S. Chen, Q. Song, Z. Zhao, Y. Liu, F. E. Alsaadi, Global asymptotic stability of fractional-order complex-valued neural networks with probabilistic time-varying delays, *Neurocomputing*, **450** (2021), 311–318. https://doi.org/10.1016/j.neucom.2021.04.043
32. J. Han, G. Chen, L. Wang, G. Zhang, J. Hu, Direct approach on fixed-time stabilization and projective synchronization of inertial neural networks with mixed delays, *Neurocomputing*, **535** (2023), 97–106. https://doi.org/10.1016/j.neucom.2023.03.038
33. A. F. Filippov, Differential equations with discontinuous right-hand side, *Mat. Sb.*, **51** (1988), 99–128.
34. G. Zhang, Y. Shen, Q. Yin, J. Sun, Passivity analysis for memristor-based recurrent neural networks with discrete and distributed delays, *Neural Networks*, **61** (2015), 49–58. https://doi.org/10.1016/j.neunet.2014.10.004
35. E. Jiménez-Rodríguez, J. D. Sánchez-Torres, A. G. Loukianov, On optimal predefined-time stabilization, *Int. J. Robust Nonlinear Control*, **27** (2017), 3620–3642. https://doi.org/10.1002/rnc.3757
36. H. Khalil, *Nonlinear systems*, 3 Eds., Prentice Hall, 2002.
37. H. Jia, D. Luo, J. Wang, H. Shen, Fixed-time synchronization for inertial cohen–grossberg delayed neural networks: an event-triggered approach, *Knowl. Based Syst.*, **250** (2022), 109104. https://doi.org/10.1016/j.knosys.2022.109104
38. F. H. Clarke, Y. S. Ledyaev, R. J. Stern, P. R. Wolenski, *Nonsmooth analysis and control theory*, Springer Science & Business Media, 1998. https://doi.org/10.1007/b97650